Allosteric Manipulation of Photoexcited State Relaxation in $(bpy)_2Ru^{II}$(binicotinic acid)

Marc W. Perkovic*

Department of Chemistry, Western Michigan University, Kalamazoo, Michigan 49008

Received March 14, 2000

The emission spectrum and luminescent lifetime of $(bpy)_2Ru^{II}$(binicotinic acid) is affected by the presence of heavy metal ions in solution. As little as 1 μM Pb^{2+} causes a red shift in emission, an increase in the emission quantum yield, and an increase in the room-temperature lifetime. A smaller red shift is observed in the 4,4′-dicarboxy analogue in the presence of large quantities of lead; however, the emission lifetime and intensity are dimished. An X-ray determination of the ground-state geometry shows that the bipyridine rings of the binicotinic acid are twisted along the 2,2′ bond by 19.3°. The interaction between lead and the binicotinic acid complex was modeled by molecular mechanics and extended Hückel calculations. The calculations show that interaction with lead flattens the bridged ring system of the binicotinic acid ligand, which affects the π^* energy levels of the ligand, the d-orbital energies of the Ru(II), and the vibrational modes available to the substituted bipyridine ligand. The inverse energy gap law behavior observed in the binicotinic acid complex is explained in terms of an allosteric interaction between lead and the binicotinic acid complex.

Introduction

Environmental signal transduction is an area of research that has received much attention in recent years. An important subclass of this work is in the area of luminescent chemical sensors.[1−3] The concept involves constructing molecules with two functional realms: (1) a detection moiety that can act as a receptor to the environmental signal and (2) a reporter moiety that will change its luminescent properties in the presence of an environmental signal. This allosterism can affect the luminophore by altering either its absorption properties or its photophysical (spectral or kinetic) properties. In the case of a transition metal complex luminophore, one may affect the emissive state by altering the electronics of the metal center, the electronics of the coordinated ligands, or both. Ruthenium(II) diimines have proved to be fertile systems for the examination of the photophysical manifestations of static ligand electronic and d-orbital effects as they pertain to signal transduction and molecular devices.[4,5] Relatively fewer investigators have examined a dynamic, or allosteric, approach to altering these same parameters.[6−9]

We report here an investigation of allosteric manipulation of excited-state behavior using $(bpy)_2Ru^{II}$(binicotinic acid). This molecule when coordinated to a $Ru^{II}(bpy)_2$ moiety fits the model sensor system described above in that it has a carboxylic acid

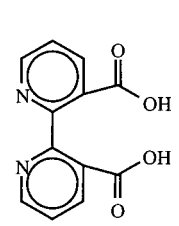

binicotinic acid
2,2'-bypiridine-3,3'-dicarboxylic acid

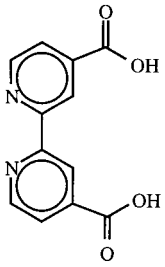

2,2'-bypiridine-4,4'-dicarboxylic acid

receptor realm attached to a well-understood reporter. Our results show that the presence of an alloster, namely, Pb(II) ions, can have a profound effect on the luminescent properties of this molecule by altering the electronics of the ligand system, by

* Phone: 616-387-2872. Fax: 616-387-2909. E-mail: perkovic@wmich.edu.

(1) Czarnick, A. W., Ed. *Fluorescent Chemosensors for Ion and Molecule Recognition*; ACS Symposium Series 538; American Chemical Society: Washington, DC, 1992.
(2) de Silva, A. P.; Gunaratne, H. Q.; Gunnlaugsson, T.; Huxley, A. J.; McCoy, C. P.; Rademacher, J. T.; Rice, T. E. *Chem. Rev.* **1997**, *97*, 1515.
(3) Wolfbeis, O. S., Ed. *Fiber Optic Chemical Sensors and Biosensors*; CRC Press: Boca Raton, FL, 1991; Vols. I and II. (b) Bissell, R. A.; de Silva, A. P.; Gunaratne, H. Q. N.; Lynch, P. L.; Maguire, G. E. M.; McCoy, C. P.; Sandanayake, K. R. A. S. *Chem. Soc. Rev.* **1992**, *21*, 187. (c) Bissell, R. A.; de Silva, A. P.; Gunaratne, H. Q. N.; Lynch, P. L.; Maguire, G. E. M.; Sandanayake, K. R. A. S. *Top. Curr. Chem.* **1993**, *168*, 223. (d) de Silva, A. P.; Gunaratne, H. Q.; Gunnlaugsson, T.; Huxley, A. J. M.; McCoy, C. P., Rademacher, J. T.; Rice, T. E. *Adv. Supramol. Chem.* **1997**, *4*, 127.
(4) Balzani, V.; Scandola, F. *Supramolecular Photochemistry*; Ellis-Horwood: Chichester, 1991. (b) Balzani, V.; Credi, A.; Scandola, F. Supramolecular Photochemistry and Photophysics. Energy-Conversion and Information-Processing Devices Based on Transition Metal Complexes. In *Transition Metals in Supramolecular Chemistry*; Fabbrizzi, L., Poggi, A., Eds.; Kluwer: Dorecht, 1994. (c) Lehn, J. M. Perspectives in Supramolecular Chemistry—from Molecular Recognition towards Molecular Information Processing and Self-Organization. *Angew. Chem., Int. Ed. Engl.* **1990**, *29*, 1304. (e) Fabbrizzi, L., Poggi, A., Eds. *Transition metals in Supramolecular Chemistry*; Kluwer: Dorecht, 1994.
(5) Henderson, L.; Fronczek, F.; Cherry, W. *J. Am. Chem. Soc.* **1984**, *106*, 5876.
(6) Szulbinski, W.; Kincaid, J. *Inorg. Chem.* **1998**, *37*, 859. (b) Sykora, M.; Kincaid, J. *Inorg. Chem.* **1995**, *34*, 5852.
(7) Bélanger, S.; Gilbeertson, M.; Yoon, D.; Stern, C.; Dang, X.; Hupp, J. *J. Chem. Soc., Dalton Trans.* **1999**, *19*, 3407.
(8) See, for example: (a) Fabrizzi, L.; Poggi, A. *Chem. Soc. Rev.* **1995**, *24*, 197. (b) Fabrizzi, L.; Licchelli, M.; Pallavicini, P.; Sacchi, D.; Taglietti, A. *Analyst* **1996**, *121*, 1763.
(9) Fernando, S.; Maharoof, U.; Deshayes, K.; Kinstle, T.; Ogawa, M. *J. Am. Chem. Soc.* **1996**, *118*, 5783.

10.1021/ic000288t CCC: $19.00
Published on Web 09/22/2000

altering the d-orbital energy levels that are important to the relaxation of the photoexcited-state species, and by affecting the molecular vibrations that are along the relaxation trajectory of the photoexcited species. Understanding the various components of excited-state relaxation affords a rational basis from which to design molecules with predictable and desired photophysical behavior.

Experimental Section

A. Syntheses. All chemicals used were of reagent grade or better and were used without further purification. 3,3-Binicotinic acid, $(bpy)_2RuCl_2 \cdot 2H_2O$, and $(bpy)_2Ru(2,2'$-bypiridine-$4,4'$-dicarboxylic acid$)^{2+}$ were prepared by literature methods.[10−12]

Preparation of $(bpy)_2Ru(3,3'$-binicotinic acid$)]PF_6$.[13] The complex was obtained by reacting 100 mg (0.2 mmol) of $(bpy)_2RuCl_2 \cdot 2H_2O$ with 50 mg (0.21 mmol) of 3,3′-binicotinic acid in ca. 25 mL of ethanol. The solution was refluxed under nitrogen for 4 h and then cooled, and the solvent was removed by evaporation under reduced pressure. The resulting solid was dissolved in ca. 20 mL of water and sorbed onto a 1.5 × 25 cm column of C-25 cation-exchange resin. The column was developed with 0.005−0.01 M HCl in water. The red-orange band was collected and the product precipitated by the addition of solid NH_4PF_6. The red solid was recrystallized from water, yield 65%.

B. Physical Measurements. 1. Spectroscopic Measurements. IR spectra were recorded in KBr pellets on a Perkin-Elmer 1710 FTIR. UV−vis spectra were recorded on a Beckman 7400 diode array spectrometer. NMR spectra were recorded on a JEOL Eclipse+ 400 multinuclear NMR (400 MHz ^1H) equipped with a *z*-axis gradient probe. Luminescence spectra were recorded on a PTI Quanta Master spectrometer. Spectra were corrected for wavelength response and lamp intensity fluctuations.

2. Photophysical Measurements. Quantum yield determinations were performed using nitrogen-purged, absorbance-matched (0.1 AU at 450 nm) samples in DMSO/water (1:1 v/v). $Ru(bpy)_3^{2+}$ was used as the standard. Luminescent lifetimes were determined by exciting the samples with the third harmonic from a Continuum Surelite-I Nd:YAG laser. The laser was run at minimum flashlamp power, and the beam was attenuated so that sample irradiation occurred with less than 100 μJ/10 ns pulse at 355 nm. The emitted light was filtered with a 450 nm cutoff filter to eliminate laser scatter and collected by a fiber optic interfaced to an Acton SP300i monochromator/Hamamatsu R928 PMT. The photomultiplier was run at a constant −1000 V, and the light level was adjusted using the monochromator slits to provide a signal no larger than 100 mV across 50 Ω. Under these conditions, no multiexponential decays that are artifacts of the PMT being driven into a nonlinear response regime were observed. Typically, 16 transients were recorded on a LeCroy LT342 DSO and the data were fit by nonlinear least-squares methods. Sample temperatures were maintained to ±0.5 K using an Oxford Optistat liquid nitrogen cryostat. All device control and data manipulations were performed with a computer program developed in-house. Variable temperature lifetime data were fit to an Arrhenius function for the determination of activation energies.

3. Electrochemical Data. Cyclic voltammograms were recorded in nitrogen-purged CH_3CN at room temperature using a BAS 50 W potentiostat equipped with Pt working and auxiliary electrodes and an $Ag/AgNO_3$ reference electrode. Tetrabutylammonium perchlorate was used as the supporting electrolyte.

4. X-ray Structure Data. Single-crystal data was recorded on a Nonius CAD4 diffractometer at room temperature using graphite-monochromated Mo Kα radiation. The crystal was mounted on a glass fiber with epoxy and placed with a random orientation on the diffractometer. The unit cell and data collection parameters were determined from 25 high-angle reflections. The space group and structural parameters were determined using the maXus[14] suite of programs. Intensity standards were recorded after each 100 min of exposure.

5. Calculations. Mechanics and electronic calculations were performed using Chem3D, SPARTAN, and CAChe.

The pH measurements were performed with a glass combination electrode on an Orion 301 pH meter.

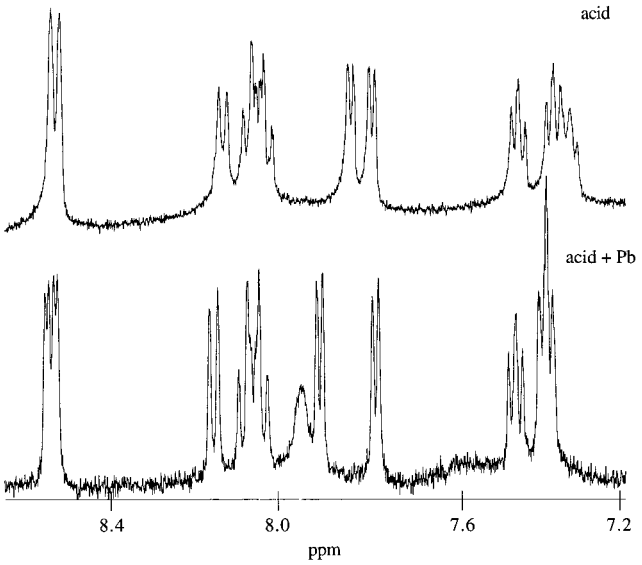

Figure 1. ^1H NMR spectrum of $(bpy)_2Ru(binicotinic\ acid)^+$ in D_2O with and without lead.

Results

Complex Preparation and Characterization. The transformation of $Ru(bpy)_2Cl_2$ to $Ru(bpy)_2(binicotinic\ acid)^{2+}$ proceeds via ligand exchange between the chlorides of the parent complex and the bidentate binicotinic acid. Ion-exchange chromatography affords efficient purification for photophysical study. The IR spectrum of the complex shows bands indicative of a carboxylic acid with a broad band at 3415 cm^{-1} (O−H) and a band at 1606 cm^{-1} (C═O). The ^1H NMR spectrum in D_2O showed resonances at 7.3 (m), 7.41 (m), 7.74 (d), 7.79 (d), 8.05 (m), and 8.5 (d) ppm, relative to DSS. These results are in accord with previous observations on a related Pt(II) complex[15] and $Ru(bpy)_3^{2+}$.[16] In the presence of 10^{-2} M $Pb(NO_3)_2$, the spectrum changed significantly, as seen in Figure 1. The multiplet at 7.3 ppm was reduced to three peaks centered at 7.3 ppm; the doublet at 8.51 became a doublet of doublets centered at 8.47, and a new broad peak was observed at 7.88 ppm. Additionally, the doublets at 7.74 and 7.79 ppm shift further apart to 7.85 and 7.75 ppm, respectively. The cyclic voltammogram (CV) of the complex in acetonitrile showed one reversible anodic wave ($Ru^{II/III}$) at +1.3 V vs $Ag/AgNO_3$, one irreversible cathodic wave at −1.3 V, and two quasireversible cathodic waves at −1.5 and −1.7 V. The CV was complicated by the appearance of a large cathodic catalytic wave beginning at −1.1 V which was likely the result of electrode binding by the binicotinic acid ligand. Compared to $Ru(bpy)_3^{2+}$, the ruthenium oxidation occurred at about 60 mV more positive and the first reduction was about

(10) Smith, G. F.; Richter, F. P. *Phenanthroline and Substituted Phenanthroline Indicators*; G. Frederick Smith Chemical Company: Columbus, 1944; p 20 ff. (b) A better route is that by Dholakia et al.: Dholakia, S.; Gillard, R. D.; Wimmer, F. L. *Polyhedron* **1985**, *4*, 791.
(11) Lay, P. A.; Sargeson, A. M.; Taube, H. *Inorg. Synth.* **1986**, *24*, 291.
(12) Johansen, O.; Kowala, C.; Mau, A. W.-H.; Sasse, W. H. F. *Aust. J. Chem.* **1979**, *32*, 1453. (b) Lay, P.; Sasse, W. H. F. *Inorg. Chem.* **1984**, *23*, 4125.
(13) Although the compound is a salt of Ru(II), our X-ray data shows that the solid is a mono-hexafluorophosphate.
(14) *maXus, a computer program for the solution and refinement of X-ray diffraction data*; MAC Science/Nonius B. V.
(15) Yoo, J.; Kim, J.-H.; Sohn, Y.; Do, Y. *Inorg. Chim. Acta* **1997**, *263*, 53.
(16) Constable, E.; Lewis, J. *Inorg. Chim. Acta* **1983**, *70*, 251.

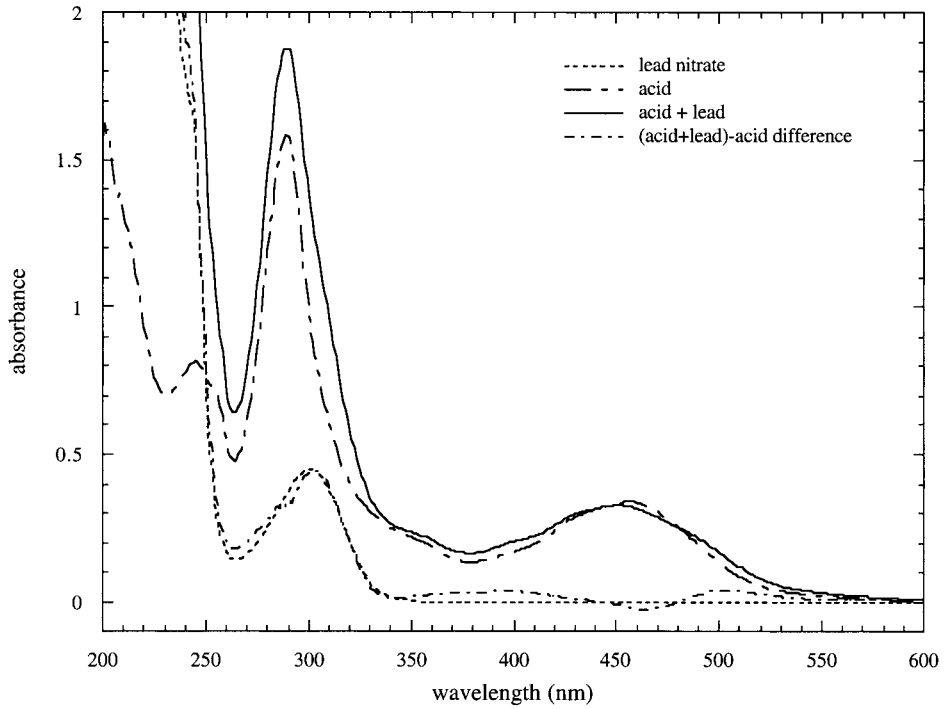

Figure 2. UV−vis spectra of the 3,3′ acid complex with and without lead in water, lead nitrate in water, and the difference spectrum between the complex with and without lead.

150 mV more positive. The UV−vis spectrum of the complex (Figure 2) in water or DMSO/water is typical of Ru(II) polypyridyls with absorption bands at 244 (254 shoulder), 288, and 455 nm. The spectrum displayed no features that changed in the presence of lead.

X-ray Determination of [Ru^{II}(bpy)$_2$(binicotinic acid)] Hexafluorophosphate. X-ray quality crystals were grown by slow evaporation from an aqueous solution of the complex and NH_4PF_6 in a refrigerator. A deep red rectangular plate, approximately 0.2 × 0.2 × 0.15 mm, was chosen by size, habit, and polarized light microscopy. The complex crystallized in the monoclinic system as a monohexafluorophosphate. The Laue symmetry was determined to be 2/*m*, and the space group was determined to be $P2_1/a$ (nonstandard setting of $P2_1/c$, No. 14)[17] by systematic absences. The data collection and refinement parameters are presented in Table 1. The structure was solved by direct methods using SIR[18] and refined in full-matrix least-squares. Lattice waters and fluorine atoms were located by difference Fourier syntheses. All non-hydrogen atoms were refined anisotropically. Hydrogens were placed in calculated positions. The largest unassigned peak in the final difference map was 1.5 e/Å^3 located near the PF_6 anion (vide infra). The next largest peak was 0.7 e/Å^3. No absorption correction was applied. The structure refined to a final *R* value of 5.7%. The refined cation is shown in Figure 3, and structural details are presented in Table 2.

There were four waters of crystallization observed. Some disorder was observed around the PF_6 anion. Attempts to account for this disorder did not significantly affect the model. As a result, the fluorines of the anion have relatively large thermal parameters in the final model and result in the largest peak observed in the final difference map. The average Ru−N bond length was 2.03 ± 0.02 Å and the N−Ru−N bond angles ranged from 78.2 to 79.0°. The angle between the planes of the two pyridine rings of the binicotinic acid was 19.3°. The closest nonbonded contact between the oxygens of the carboxyl groups was 2.9 Å, which may indicate at least weak hydrogen bonding. No hydrogen was visible in the electron density maps near the carboxyl oxygens. The entire binicotinic acid ligand is tipped by ∼3.5° relative to the other trans N−Ru−N bypyridine planes. The angle between the other pyridine rings in the bpy ligands is 4 ± 2°.

Table 1. Data Collection and Refinement Parameters for [(bpy)$_2$Ru(binicotinic acid)·4H$_2$O]PF$_6$

space group	$P2_1/a$
cell constants	$a = 12.1028(0.0026)$ Å
	$b = 14.6017(0.0032)$ Å
	$c = 19.8800(0.0036)$ Å
	$\beta = 102.6826(0.0161)°$
reflections collected	$-14 < h > 14$
	$-17 < k > 0$
	$0 > l > 23$
no. of refl. (total/unique/$I_0 > 3\sigma(I_0)$)	7006/6556/3150
scan method	$\omega/2\theta$
mol formula	$C_{32}H_{33}O_9N_6RuPF_6$
formula weight	890.63 amu
formula units per cell	$Z = 4$
density	$d_{calc} = 1.730$ g/cm^3
abs. coef.	$\mu = 6.15$ cm^{-1}
temperature	$T = 295$ K
radiation (Mo Kα)	$\lambda = 0.7107$ Å
F_{000}	1684 e
structural parameters/refined	653/487
R^a	0.0597
$R_w{}^b$	0.0574
weights	$w = \sigma(F)^{-2}$

$^a R = \sum ||F_o| - |F_c||/\sum |F_o|$. $^b R_w = [\sum w(|F_o| - |F_c|)/\sum w|F_o|^2)]^{1/2}$.

Photophysical Measurements. The steady-state luminescence spectrum of the binicotinic acid complex at room temperature shows a typical ruthenium(II) polypyridyl emission (Figure 4). There was a slight pH dependence in the emission

(17) *International Tables for X-ray Crystallography*; Kynoch: Birmingham, 1965.
(18) SIR92: Altomore, A.; Casscarano, G.; Giacovazzo, C.; Guggliandi, A.; Burla, M. C.; Polidori, G.; Camalli, M. *J. Appl. Crystallogr.* **1994**, *27*, 435.

Table 2. Selected Bond Lengths (Å) and Angles (deg)[a]

bond lengths			
Ru(1)−N(30)	2.04131(7)	Ru(1)−N(20)	2.0543(8)
Ru(1)−N(31)	2.0336(8)	Ru(1)−N(21)	2.0708(8)
Ru(1)−N(10)	2.0538(8)	Ru(1)−N(11)	2.0587(9)
N(30)−C(30)	1.329(1)	N(30)−C(34)	1.380(1)
N(20)−C(24)	1.373(1)	N(20)−C(20)	1.323(1)
O(2)−C(40)	1.266(1)	N(31)−C(35)	1.407(1)
N(31)−C(39)	1.326(1)	N(21)−C(29)	1.348(1)
N(21)−C(25)	1.388(1)	O(3)−C(41)	1.203(1)
N(10)−C(10)	1.356(1)	N(10)−C(14)	1.366(1)
N(11)−C(15)	1.366(1)	N(11)−C(19)	1.368(1)
C(35)−C(36)	1.400(1)	C(35)−C(34)	1.500(1)
O(4)−C(41)	1.313(1)	C(30)−C(31)	1.362(1)
O(1)−C(40)	1.253(1)	C(39)−C(38)	1.364(1)

bond angles			
N(30)−Ru(1)−N(20)	95.3(1)	N(30)−Ru(1)−N(31)	78.2(1)
N(30)−Ru(1)−N(21)	174.0(1)	N(30)−Ru(1)−N(10)	94.6(1)
N(30)−Ru(1)−N(11)	90.0(1)	N(20)−Ru(1)−N(31)	90.5(1)
N(20)−Ru(1)−N(21)	79.0(1)	N(20)−Ru(1)−N(10)	98.5(1)
N(20)−Ru(1)−N(11)	174.2(1)	N(31)−Ru(1)−N(21)	99.7(1)
N(31)−Ru(1)−N(10)	168.9(1)	N(31)−Ru(1)−N(11)	92.9(1)
N(21)−Ru(1)−N(10)	88.3(1)	N(21)−Ru(1)−N(11)	95.7(1)
N(10)−Ru(1)−N(11)	78.6(1)		

[a] An ORTEP diagram with the complete atom numbering scheme is available as Supporting Information.

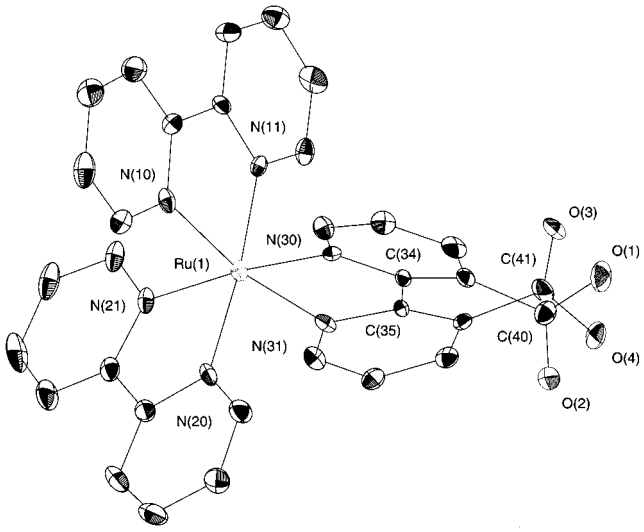

Figure 3. ORTEP diagram of the $(bpy)_2Ru(binicotinic\ acid)PF_6 \cdot 4H_2O$ cation.

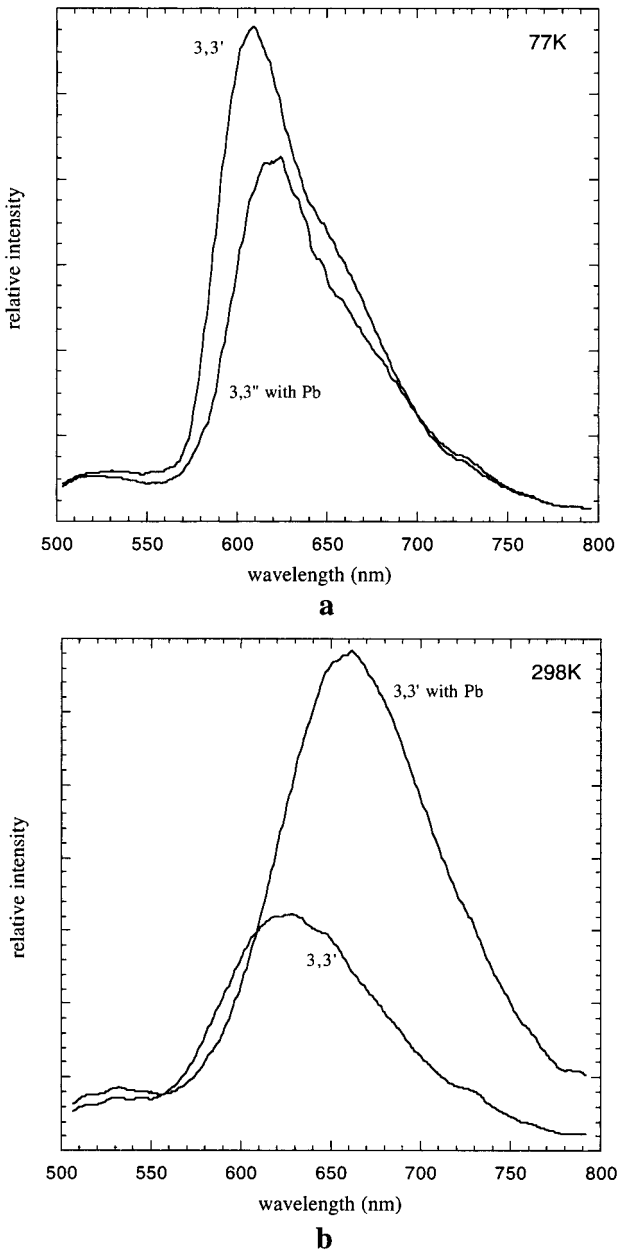

Figure 4. Luminescence spectra of absorbance-matched samples of the 3,3′ complex at (a) 298 K and (b) 77 K in DMSO/water (1:1 v/v).

spectrum in the range of pH = 2−11, and this pH effect was entirely manifested in changes in emission intensity in this range. There was no spectral shift observed.[25] A plot of emission intensity versus pH showed only one transition at pH = 3.5. The spectrum in a constant ionic strength buffer (1 M, pH = 7) or DMSO/buffer solution showed a room-temperature emission maximum at 655 nm. In the presence of as little as 100 μM Pb^{2+} (as the nitrate), the emission spectrum underwent a bathochromic shift and an increase in emission intensity that was $[Pb^{2+}]$ dependent. The maximum spectral shift observed resulted in a λ_{max} of 683 nm at 0.1 M $Pb(NO_3)_2$. The spectral shift was monotonic in $[Pb^{2+}]$. The emission intensity rose with $[Pb^{2+}]$ to a maximum value of $\phi/\phi_{Pb} = 2.7$ at 0.01 M $Pb(NO_3)_2$, and then dropped off as the lead was increased another 10-fold. The intensity diminution at high $[Pb^{2+}]$ is the result of a $Pb(NO_3)^{2+}$ inner filter effect on the excitation. The binicotinic acid complex shows essentially no effect in the presence of the similarly sized[19] Ca^{2+}, and $Ru(bpy)_3^{2+}$ shows no change in emission behavior in the presence of Pb^{2+} or Ca^{2+}. Cadmium(II) and mercury(II) show a similar, although smaller, effect compared to that of lead. We did not expect this molecule to exhibit any alloster selectivity, and we are currently investigating the source of this selectivity.[20] At 77 K, the binicotinic complex had a featureless emission spectrum with a maximum at 615 nm in lead-free DMSO/buffer, which shifted to 635 nm in DMSO/buffer/0.01 M Pb^{2+}. In absorbance-matched samples at 77 K, the alloster mixture had a smaller emission yield than the alloster-free complex (Figure 4).

The excited-state lifetime of the binicotinic acid complex at 77 K was 2.9 μs in lead-free solution and dropped slightly to 2.4 μs in the presence of 10^{-2} M Pb^{2+}. At room temperature, the observed lifetime was 29.3 ns, which rose to 170 ns when lead was present. These changes in observed lifetime track the emission quantum yields (Table 3). The activation energies

(19) Huhey, J.; Keiter, E.; Keiter, R. *Inorganic Chemistry-Principles of Structure and Reactivity*; Harper Collins: New York, 1993.
(20) Lyuk, A.; Constales, C.; Perkovic, M. W. Work in progress.

Table 3. Photophysical Data

complex	λ_{max}^{77K} (nm)[d]		τ_{77} (μs)		ϕ_{77} [f]		λ_{max}^{298K} (nm)[d]		τ_{298} (ns)		ϕ_{298} [f]	
	w/o Pb	w/ Pb[e]	w/o Pb	w/ Pb	w/o Pb	w/ Pb	w/o Pb	w/ Pb[e]	w/o Pb	w/ Pb	w/o Pb	w/ Pb
$(bpy)_2Ru$(binicotinic acid)$^{+}$ [a]	610	623	2.9	2.4	0.37	0.3	655	683	29.3	170	0.04	0.11
$(bpy)_2Ru$(4,4′-diacid)$^{2+}$	608	608	6.1	6.2			670	685	465	395	0.86[g]	0.71
$Ru(bpy)_3^{2+}$	580		5.2		1		610	610	630	630	1	1
$(bpy)_2Ru(daf)^{2+}$ [b]	574		5.9		1.7						0.02	
$Ru((CH_2)_2(bpy))_3^{2+}$ [c]			5.4						630			
$Ru((CH_2)_3(bpy))_3^{2+}$ [c]			2.7						455			

[a] Complex in DSMO/buffer. [b] From ref 5. daf = diazafluorene. [c] From ref 27. These complexes are 2,2′-bipyridine bridged via methylenes at the 3,3′-position. [d] Emission max from this work ±2 nm. [e] Maxima are reported at 1×10^{-2} M $Pb(NO_3)_2$. [f] Quantum yield values from corrected spectra reported to ±10% against $Ru^{II}(bpy)_3$. [g] From ref 12b.

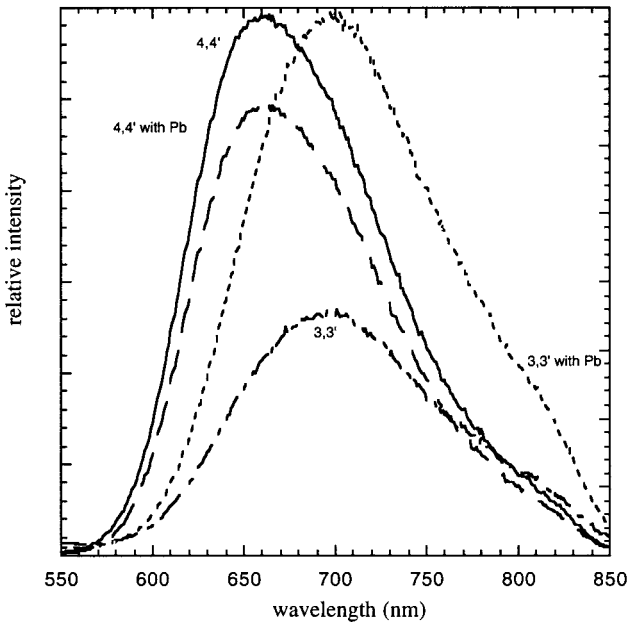

Figure 5. Luminescence spectra of 3,3′ and 4,4′ complexes in 2 M buffer at pH 7.5, with and without lead. The *y* axes are normalized for each complex pair.

obtained from variable temperature lifetime measurements were 1466 and 1526 cm^{-1} with preexponential factors of 8.9×10^9 and 1.1×10^{10} without and with lead, respectively.

We also examined the analogous $(bpy)_2Ru^{II}$(2,2′-bipyridine-4,4′-dicarboxylic acid) complex. When in the presence of relatively high (ca 10^{-1} M) lead nitrate, the room-temperature emission spectrum of this complex shifted to the red by 15 nm. Unlike the binicotinic acid complex, however, the emission intensity was accompanied by a decrease in intensity rather than the increase with $\phi/\phi_{Pb} = 0.86$. In accordance with the energy gap law and the observed intensity change, the excited-state lifetime of the complex decreased from 465 ns in lead-free solution to 395 ns in 10^{-1} M $Pb(NO_3)_2$. The NMR spectrum of the 4,4′-dicarboxylic acid complex in D_2O showed essentially no change in the ^1H NMR spectrum in the presence of lead.

When both the 3,3′ and 4,4′ complexes were examined in high ionic strength (>2 M) buffers at pH > 7, the spectral change associated with the presence of lead disappeared in the 4,4′ complex and was very small (~10 nm) in the 3,3′ complex; however, the respective changes in emission intensity were still observed (Figure 5).

Discussion

Preparation and characterization of the title complex was straightforward, and the results were typical for a Ru(II) diimine complex. What is striking about this system is the degree to which adding a photophysically benign ion such as Pb^{2+} to the solution affects the photoexcited-state behavior of the complex. It is clear that there are several factors at play because we see such different behavior between the 3,3′ and 4,4′ complexes. The behavior of the 4,4′ complex is similar to that observed when the carboxylates are protonated or deprotonated.[12] In this case, the redistribution of electron density in the diimine ligand is manifested in the red shift and decrease in emission intensity. The behavior of the 3,3′ complex is more complicated. Indeed, there is a similar electronic effect occurring in that the complex demonstrates a similar red shift in emission. However, the shift is much larger in the 3,3′ complex, and the photophysical behavior is contrary to the observed spectral behavior. One expects that as the emission shifts to the red there should be a concomitant decrease in excited-state lifetime. This is not observed. We postulate that introducing Pb^{2+} into solution with the 3,3′ complex results in an allosteric interaction that alters the geometry of the binicotinic acid ligand in such a way as to affect its electronics; the electronics of the Ru(II) and molecular motions accessible to the ligand are important to thermally activated relaxation of the photoexcited state. The most reasonable motion to examine is twisting of the two pyridine rings along the 2,2′ bond of the binicotinic acid, which will draw the two rings toward coplanarity upon coordination between a lead ion and the carboxyl groups of the complex. This motion is also in accord with our observations on the ground-state and excited-state behavior of the 3,3′ complex. Calculations of the ground-state geometry of the ligands show that in the case of the 4,4′ diacid, the closest oxygen−oxygen contact is 6.3 Å, too distant to chelate an allosteric ion. In contrast, the 3,3′ complex has an oxygen−oxygen contact of 2.8 Å and thus would be capable of coordinating to lead. This O−O contact was confirmed in the X-ray analysis (vide infra).

Our observation of the pK_a (~3.5) for the 3,3′ complex falls into the same range as that of the 4,4′ complex, which was reported to have $pK_{a1} = 3.6$ and $pK_{a2} = 4.5$ for the stepwise deprotonation of the carboxyls.[12] The fact that we observe only a single deprotonation step is a matter of either the insensitivity of our measurement or a relatively low pK_{a1} for this complex, leveled by water. Because the crystal grown for the X-ray analysis was the monodeprotonated form, we can presume with reasonable confidence that pK_{a1} is fairly small in this complex. Most germane, though, is that at pH ≥ 7 the dominant species in solution is the one with both carboxylic acids deprotonated. This is significant because we need not worry about the association of a +2 alloster with a potentially +2 ruthenium complex but rather about the association of a +2 alloster with a neutral molecule. Thus, the electrostatic repulsions that one expects are significantly smaller. Because the lead concentrations necessary to induce an effect were typically 1000−10000 times greater than the concentration of the ruthenium complex, we

can assume that the equilibrium constant for the Ru(diacid)−alloster complex is small. This will become a larger issue as we prepare ligand systems with more specific alloster binding characteristics. At the moment, we are most concerned with the source of the divergent photophysical behavior of the 3,3′ and 4,4′ ruthenium complexes. Because all of the measurements were performed in high ionic strength, buffered solution, there is no reason to suspect that the species being investigated is undergoing acid/base chemistry when lead is introduced into solution.

Attempts at growing crystals of the complex−alloster mix so far have failed; however, the ground state structure of the title complex offers some insights into our postulated mechanism. The monodeprotonated form of the molecule seems to be the common isolable form, judging by the broad, relatively low-frequency C═O stretch in the IR spectrum and the observation of a monohexafluorophosphate X-ray structure. The C═O stretch is suggestive of a form consisting of one carboxylate and one carboxylic acid. The 19.3° twist of the binicotinic acid pyridine rings is the result of steric repulsion between the two CO_2 moieties. The closest nonbonded contact between the oxygens of the CO_2 groups was 2.9 Å, which may indicate at least weak hydrogen bonding that may offset the steric repulsion between the two groups. No hydrogen was visible in the electron density maps near the carboxyl oxygens, but this is not surprising in a heavy atom structure. Perhaps to compensate for the loss of angular overlap between the nitrogens on the binicotinic acid and the ruthenium ion as a result of the twist, the entire ligand is tipped by ∼3.5° relative to the other trans N−Ru−N bypyridine planes. Ruthenium bipyridine complexes that have at least one sterically stressed bipyridine have shown similar distortions. For example, the $(bpy)_2$Ru(3,3′-annealated bipyridine)$^{2+}$ with four methylene units bridging the two rings at the 3,3′ position had an inter-ring angle of 30.4°,[23] and Ru(3,3′-diamino-2,2′- bipyridine)$_3^{2+}$ had inter-ring angles that spanned the range from 7.3 to 17.3°.[21] The structure of Pt(binicotinic acid)$(Cl_2)\cdot$DMF[15] showed a larger twisting of the pyridine rings of the binicotinic acid ligand of 26.5°. The authors of the Pt work did not examine the orientation of the Cl−Pt−Cl plane relative to the N−Pt−N plane; however, their description of the dihedral angles containing Cl−Pt−N moieties suggests that there may be a similar tipping of the entire ring system as is observed in the Ru(II) structure presented here. The twisting of the bipyridine rings was attributed to steric repulsion caused by the carboxyls at the 3,3′ positions of the acid ligand.[15] Similar results have been observed for the analogous Cu(II) complex.[22] In both the Pt and Cu systems, however, neither carboxyl is deprotonated. This observation may be attributed to the difference in the electron density that each ring would experience, manifested in the pK_a of the carboxylic acid, as a result of being bonded to a metal with a +2 charge, in the case of Ru(II), as opposed to the metals with essentially zero charge in the complexes with metal−halide bonds.

The ^{1}H NMR spectrum of the 3,3′ complex shows features consistent with a 2,2′ interpyridine twist. Modeling suggests that the two protons most affected by such a ligand motion will be the protons α to the binicotinic acid nitrogen and those α to the binicotinic acid carbonyls (the 4 and 6 positions). The former will experience a different inductive field from the adjacent π systems of the bipyridine ligands, and the latter a different field from the electrons in the C═O double bond. These changes in the NMR spectrum agree with what has been observed in 2,2′-bipyridine complexes in which an intra-pyridine deformation was induced synthetically.[23] Uncoordinated binicotinic acid in D_2O does not show the same allosteric effect with lead or any other cations examined. This is the result of the two carboxylic acids orienting trans with respect to one another because of steric repulsion,[24] further stabilized by hydrogen bonding with the solvent. When complexed to Ru(II), however, the two carboxyls are forced into a geometry more conducive to a bidentate interaction with an alloster. The 4,4′ complex showed no change in the NMR spectrum in the presence of lead.

The absorption spectrum of the binicotinic acid complex has bands that are attributed to intraligand ($\pi-\pi^*$) transitions in the case of the UV absorptions and to a metal-to-ligand charge transfer (MLCT) (d−π^*) in the case of the 455 nm peak. The spectrum was qualitatively identical to that of Ru$(bpy)_3^{2+}$ and showed no features attributable to the presence of the carboxyl groups on the binicotinic acid. As has been observed with other acid derivatives, the absorption spectrum demonstrated a pronounced pH dependence.[12,25] The UV absorptions of the 3,3′ complex showed no spectral change upon addition of Pb^{2+} to the solution when corrected for the absorption due to $Pb(NO_3)_2$, but the 455 nm peak showed a slight red shift to 460 nm. The ca. 10% increase in intensity of the 288 nm band may be a result of not completely correcting for the background lead absorbance. Similarly, the 244 nm band is obscured by the lead. The allosteric interaction between lead and the binicotinic acid ligand is expected to have the largest effect on the N−Ru−N geometry (dπ orbitals) and the π^* energy level of the aromatic carboxyl system (vide infra). A much smaller effect is expected on the intraligand UV transitions, and such has been observed in similarly distorted systems.[5,23] That a twist of the binicotinic acid system is occurring when lead is introduced into solution of the 3,3′ complex is clear. How this change may affect the luminescent behavior of the complex is less clear.

The changes in luminescent behavior can be examined by considering three features important to excited-state relaxation: (1) the energy of the lowest unoccupied molecular orbital (LUMO) of the binicotinic acid ligand; (2) the d-orbital overlap with the donor nitrogens of this ligand, and (3) changes in the accessible vibrational modes. We have modeled the behavior of the free binicotinic acid by molecular mechanics and extended Hückel electronic calculations. The lowest energy conformation of the free ligand has the carboxyls cis with respect to the 2,2′ bipyridine bond with a dihedral angle of 60 ± 5° (the steric energy surface is rather shallow near its minimum). Upon coordination of two or three[26] of the carboxyl oxygens to a Pb^{2+} ion, the inter-ring angle is lowered by 13° to 47.2 ± 3°. An extended Hückel calculation reveals that the LUMO of the binicotinic acid ring system is lowered by 537 cm^{-1} by this distortion. This is in remarkably good agreement (a factor of 2 or so) with the observation, considering that one expects a

(21) Araki, K.; Fuse, M.; Kishii, N.; Shiraishi, S. *Bull. Chem. Soc. Jpn.* **1990**, *63*, 1299.
(22) Goddard, B.; Hemalatha, B.; Rajasekharan, M. *Acta Crystallogr., Sect. C* **1990**, *46*, 33.
(23) Thummel, R.; Lefoulon, F.; Korp, J. *Inorg. Chem.* **1987**, *26*, 2370.
(24) This is similar to what has been observed by Rebek in crown ether analogues; see: Rebek, J.; Trend, J.; Wattley, R.; Chakravorti, S. *J. Am. Chem. Soc.* **1979**, *101*, 4333.
(25) See, for example: (a) Montalalti, M.; Wadhwa, S.; Kim, W. Y.; Kipp, R. A.; Schmehl, R. H. *Inorg. Chem.* **2000**, *39*, 76. (b) Ferguson, J.; Mau, A. W.-H.; Sasse, W. H. F. *Chem. Phys. Lett.* **1979**, *68*, 21. (c) Nazeeruddin, Md. K.; Zakeerudin, S. M.; Humphry-Baker, R.; Jirousek, M.; Liska, P.; Vlachopoulos, N.; Shklover, V.; Fischer, C. H.; Grätzel, M. *Inorg. Chem.* **1999**, *38*, 6298. (d) Hicks, C.; Fan, J.; Rutenberg, I.; Gafney, H. D. *Coord. Chem. Rev.* **1998**, *171*, 71. (e) Vos, J. G. *Polyhedron* **1992**, *18*, 2285 and references therein.
(26) To coordinate a tetrahedral hydrated Pb^{2+} ion, the geometry of the oxygens on the two carboxyls falls between these limits.

concomitant change in the d-orbital energies because of the increased angular overlap as the rings twist toward greater coplanarity. Such a motion should result in an increase in ligand field strength of the binicotinic acid when lead is coordinated at the carboxyls.[5,23] These results are qualitatively similar to what was observed by Thummel et al.[27] in a series of substituted bipyridines. In that study, a series of 2,2′-bipyridine ligands were prepared with methylene linkages of varying lengths at the 3,3′ position. As the length of the methylene chain was altered, so too was the degree to which the inter-pyridine ring planarity was affected and, as a consequence, the emission maximum. That study is not entirely comparable because those investigators examined tris complexes that lacked two normal bipyridines. Nevertheless, the red shift in emission is understandable, but it is in conflict with the resulting larger room-temperature lifetime of the excited state in the alloster mixture.

The observed larger activation energy for the alloster mixture is qualitatively in accord with the widely accepted model for electronic relaxation in Ru(II) diimines, that is, that an increase in the energy of the d-orbital manifold will retard the nonradiative rate. Kincaid has examined the photophysical behavior of MLCT excited states entrapped in zeolite cages[6] where interactions between the cage and the photoexcited complex result in changes in ligand π^* and substituted bipyridine ligand field strength similar to what we observe. However, unlike that case, we do not see evidence for the so-called 4th MLCT state. We should also note that we observe no net photochemistry when lead is present in solution with the binicotinic acid complex. Furthermore, a change in activation energy with and without lead of only 60 cm^{-1} is sufficiently small relative to kT at room temperature that ^{3}MLCT$-^3$dd equilibrium is inadequate to account for the observed behavior. Some clues may be garnered from the luminescence spectrum of the complex. Although we did not perform any spectral fitting, it is reasonable to assume that the electronic origin of the emission is the same at 77 K and room temperature. The large increase in emission yield for the room-temperature emission then is vibronic in nature. Resonance Raman studies of 3,3′-polymethylene-bipyridine complexes have shown that relatively low-frequency vibrations (such as twisting about the 2,2′ bond) in bipyridine ligands is an important vibrational mode in electronic relaxation.[27] In cases where the available twisting amplitude was small, for example, because of a short methylene bridge, or interaction with a zeolite cage, ligand field effects dominated. However, when the bridge length was large enough to mitigate the ligand field effects (increase the inter-ring angle), the flexibility of the bridge results in the vibronic component becoming more important. In the case at hand, coordination of lead at the carboxyls of binicotinic acid results in both a larger ligand field of the binicotinic acid ligand and a restriction in the ability of the ligand to twist along the 2,2′ bond. Thus, at low temperature where insufficient thermal energy limits the nonradiative channels, the lower π^* energy of the binicotinic acid is manifested in the red-shifted emission and a shorter lifetime in accord with the energy gap law. At high temperature, these effects are offset by the presence of lead, which restricts the vibrational modes available to the binicotinic acid ligand, thus reducing this important contribution to k_{nr}.

We have examined how allosteric interactions can influence the photoexcited state behavior of a transition metal luminophore. The exact mechanism of the effect is still not entirely clear, but experimental results demonstrate that the alloster may restrict ligand motions that are important for excited-state relaxation. We are currently examining other alloster−acceptor systems and synthetically induced twisted systems with more and less rigid spacers to further investigate these effects.

Acknowledgment. The author thanks Ms. Consuala Constales and Ms. Anastasia Lyuk for repeating many of the luminescence measurements and Professor D. Paul Rillema of Wichita State University and Dr. Youxaing Wang whose observations on the pH behavior of the 3,3′ diacid complex stimulated this work. Financial assistance was provided by the National Science Foundation (Grant No. CHE-9876142). The author also thanks the Camille and Henry Dreyfus Foundation and the Kalamazoo Foundation for their generous support.

Supporting Information Available: An ORTEP diagram with the complete atom numbering scheme for $Ru^{II}(bpy)_2$(binicotinic acid) and tables containing data for fractional atomic coordinates, anisotropic thermal parameters, intramolecular bond lengths and angles, intramolecular torsion angles, and intermolecular nonbonded distances. This material is available free of charge via the Internet at http://pubs.acs.org.

IC000288T

(27) Strekas, T.; Gafney, H.; Tysoe, S.; Thummel, R. *Inorg. Chem.* **1989**, *28*, 2964.